Jurnal Teknologi

Full Paper

SEISMIC WAVE TIME OF ARRIVAL AND PATH VELOCITY ESTIMATION USING 1-Hz GPS DATA

Mohd Azizi Alim Shah[a], Wan Anom Wan Aris[a*], Ahmad Zuri Sha'ameri[b], Tajul Ariffin Musa[a], Shahidatul Sadiah Abdul Manan[b], Muhammad Hafiz Mohd Yatim[a]

[a]Faculty of Built Environment and Surveying, Universiti Teknologi Malaysia, 81310 UTM Johor Bahru, Johor, Malaysia
[b]School of Electrical Engineering, Faculty of Engineering, Universiti Teknologi Malaysia, 81310 UTM Johor Bahru, Johor, Malaysia

Article history
Received
23 September 2022
Received in revised form
23 July 2023
Accepted
6 August 2023
Published Online
20 October 2023

*Corresponding author
wananom@utm.my

Graphical abstract

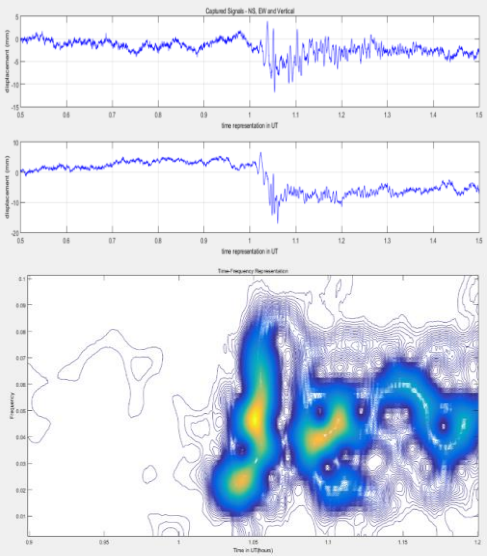

Abstract

This paper proposed the method of determining seismic wave TOA and path velocity from Global Positioning System (GPS) data. High-rate GPS data from 13 Continuous Operational Reference Station (CORS) were utilized to obtain displacement and seismic waveform during the occurrence of Sumatra-Andaman 9.2Mw earthquake 2004. To detect seismic body waves using GPS data is difficult because of attenuated signal, therefore seismic surface waves have been used. The seismic wave TOA of between 116 s to 194 s was determined using time-frequency representation (TFR). The estimated seismic wave path velocities were found within the range of 3.8 km/s to 4.6 km/s, indicated as secondary wave or surface wave. To validate the estimated path velocity, it was compared with other research with an average value of 6 km/s to 13 km/s for body wave and 2 km/s to 5 km/s for surface wave. These results indicate that GPS CORS can be an alternative sensor for detecting earthquakes other than seismometers.

Keywords: Earthquake, High-rate GPS, Seismic wave, TOA, Path velocity

Abstrak

Kertas kerja ini mencadangkan kaedah penentuan TOA gelombang seismik dan halaju laluan daripada data Global Positioning System (GPS). Data GPS berkadar tinggi daripada 13 Stesen Rujukan Operasi Berterusan (CORS) telah digunakan untuk mendapatkan anjakan dan bentuk gelombang seismik semasa berlakunya gempa bumi Sumatera-Andaman 9.2Mw 2004. Untuk mengesan gelombang badan seismik menggunakan data GPS adalah sukar kerana isyarat yang dilemahkan, oleh itu gelombang permukaan seismik telah digunakan. Gelombang seismik TOA antara 116 s hingga 194 s ditentukan menggunakan perwakilan frekuensi masa (TFR). Anggaran halaju laluan gelombang seismik ditemui dalam julat 3.8 km/s hingga 4.6 km/s, ditunjukkan sebagai gelombang sekunder atau gelombang permukaan. Untuk mengesahkan anggaran halaju laluan, ia dibandingkan dengan penyelidikan lain dengan nilai purata 6 km/s hingga 13 km/s untuk gelombang badan dan 2 km/s hingga 5 km/s untuk gelombang permukaan. Keputusan ini menunjukkan bahawa GPS CORS boleh menjadi sensor alternatif untuk mengesan gempa bumi selain daripada seismometer.

Kata kunci: Gempa bumi, GPS kadar tinggi, Gelombang seismik, TOA, Halaju laluan

1.0 INTRODUCTION

The Sumatra Andaman earthquake in December, 2004 is considered as the largest earthquake in Southeast Asia. This earthquake contributed to momentous crustal deformation in spatial sense over broad area causing fatal tsunami [32, 38]. It is noted that high distribution of seismometer stations in Southeast Asia can be used for contributing earthquake information [9, 14, 24]. There have been several studies conducted to re-compute the aforementioned earthquake epicenter and strength by using the GPS network in Sumatra Indonesia [3]. However, challenge has arisen in the need of far-field regional-based ground acceleration information, which can possibly be measured from Peninsular Malaysia and Borneo regions.

The use of GPS has become a vital tool to study long term crustal deformation through coordinate time series (CTS) of daily solution [11, 34]. Nowadays, the development of GPS instrumentation, data storage and GPS processing have enabled the high sampling rate of coordinate time series. This improvement has increased the sensitivity of GPS receiver to act as seismometer that is able to provide ground acceleration information from this high-rate coordinate time series [18]. This GPS is expected to provide far-field ground shaking information from high-rate CTS, thus improving the earthquake information.

Several studies described the use of high-rate GPS data in monitoring seismic deformation [20, 21]. The high-rate GPS data can capture rapid co-seismic ground displacements over a range of frequencies and amplitudes that are wider compared to what seismic sensors can do [5, 18]. Several researchers have utilized high-rate GPS to detect seismic wave. For example, Geng *et al. (2016)* carried out an investigation to capture seismic wave using high-rate multi GNSS in 2015 Nepal earthquake, the 2013 Lushan earthquake [37] and 2017 Mexico earthquake [36].

With the assistance of GPS measurements, tectonic displacement due to earthquake, also known as seismic wave, can be analysed by generating CTS [12]. The seismic wave can be used to obtain information of seismic wave characteristics such as seismic wave TOA and path velocity [37]. However, seismic wave time of arrival is difficult to estimate particularly the small and weak seismic wave [33]. Accurate detection of seismic wave TOA as well as path velocity estimation are important for estimation of earthquake's epicenter [27, 36]. In this study, TFR method was applied to estimate seismic wave TOA in the time-frequency domain. The path velocity can be inversely estimated by using the TOA and distance between CORS and earthquake's location [27].

This paper provides insight into seismic wave TOA and path velocity analysis using GPS CORS network in Malaysia. Section 2 discusses the data sets and methodology. In Section 3, results of CTS displacement, seismic wave TOA detection and estimation of seismic path velocity are discussed. Lastly, in section 4, the conclusion and recommendation are presented.

2.0 METHODOLOGY

This section discusses the GPS data and methodology for estimating seismic wave TOA and path velocity. Figure 1 shows the methodology of this study.

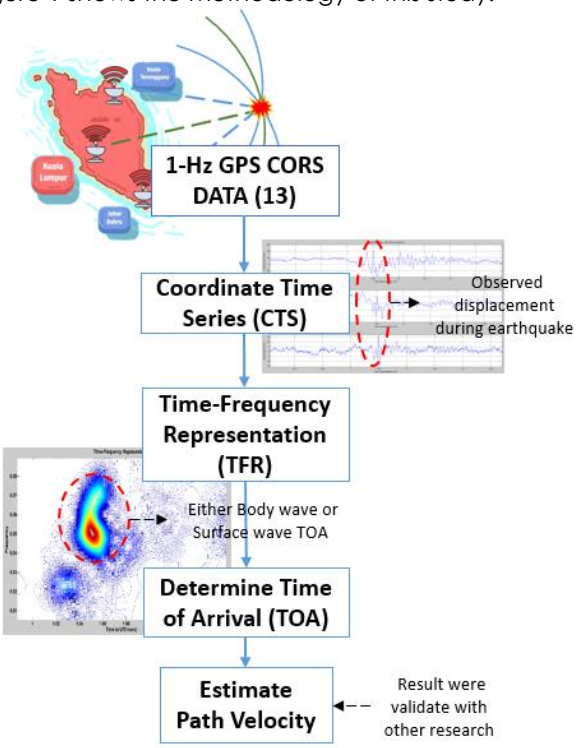

Figure 1 Methodology of this study

2.1 GPS Data

The GPS CORS stations are considered as far-field stations due to the distance that is around 300-1100 km from the earthquake's epicenter [6]. 1 hour of GPS data on 26th December 2004 with 1-Hz sampling rate as recorded by 13 GPS CORS network in Peninsular Malaysia was utilised in this study, consisting of Malaysia Network Real-Time kinematic (MyRTKnet) and Malaysia Active GPS system (MASS) [1]. Each GPS CORS distance to the epicentre ranges from 517.78 km to 925.33km as illustrated in Figure 2.

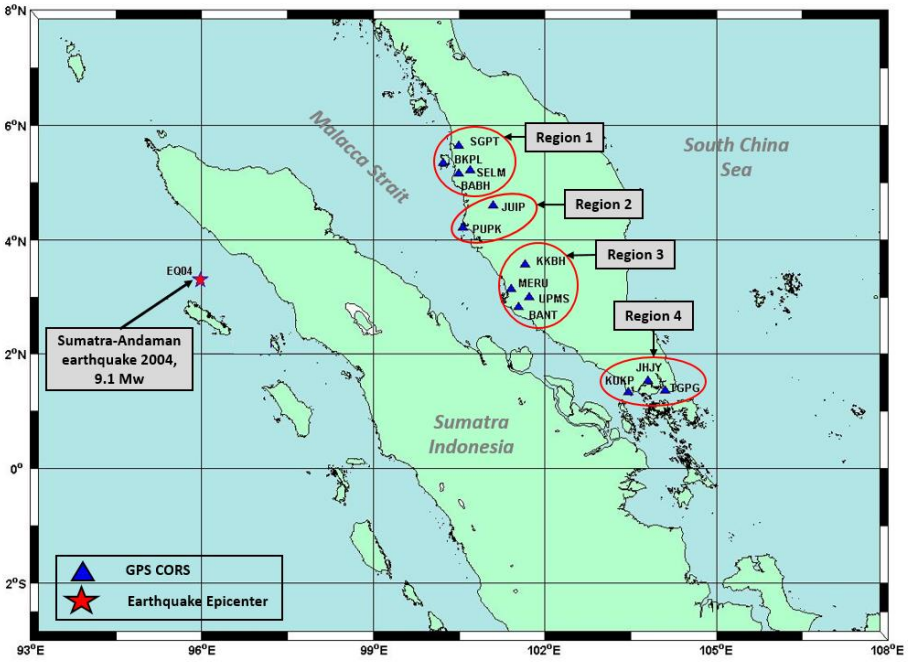

Figure 2 Distribution of GPS CORS station and location of earthquake epicenter

These 13 GPS CORS stations were divided into 4 regions. Region 1 covers northern part of Peninsular Malaysia between the latitude of 5.20° - 5.50°. Region 2 is between the latitude of 4.12° - 4.36°. Region 3 coverage is eastern Peninsular Malaysia with the latitude of 2.49° - 3.33°. Region 4 coverage in southern Peninsular Malaysia is between the latitude of 1.19° - 1.32°. According to other research, the geological structure of this region consists of siltstone, mudstone, sandstone and limestone properties [31]. Table 1 summarises the selected GPS CORS based on the 4 regions.

Table 1 Selected GPS CORS based on 4 Regions

Region	Coverage (latitude)	Selected MyRTKnet
Region 1	5.20° - 5.50°	BKPL, SELM, SGPT, BABH
Region 2	4.12° - 4.36°	PUPK, JUIP
Region 3	2.49° - 3.33°	MERU, BANT, UPMS, KKBH
Region 4	1.19° - 1.32°	KUKP, JHJY, TGPG

In order to ensure the precision of CTS, scientific software Bernese 5.2 was utilised to handle the GPS measurement error by applying ambiguity resolution strategy. Table 2 summarises the processing parameter and model that were applied in the GPS processing.

Table 2 Parameters and models for GPS data processing

Processing Parameter	Processing Strategy
Input data	Daily
Elevation cut off angle	5°
Sampling rate	1 seconds
Orbit/EOP	International GNSS service (IGS) final orbits (SP3) and Earth orientation Parameter (EOP)
Reference frame	Constrained to ITRF2008 reference frame
Ocean loading model	FES2014b
Ionosphere	Double difference ionosphere free (IF) Linear combination (L3)
Ambiguity solution	Fixed, resolved using QIF strategy with baseline < 2000 km

2.2 Time frequency Analysis

Time-frequency analysis provides accurate time and frequency parameter from estimation of true signal characteristic. The spectrogram which belongs to class of quadratic time-frequency distribution was utilized and can be expressed as follows [2]:

$$\rho_x[n,k] = \left| \sum_{\lambda=0}^{M-1} w[\lambda - n]\, x[\lambda]\, e^{-j2\pi k\lambda/M} \right|^2 \quad (1)$$

where $w[n]$ is the window function, M is the window length and $x[n]$ is the signal of interest.

To determine the quality of the acquired signal, the signal-to-noise ratio (SNR) is often used to minimise the error. Based on *Sha'ameri et al. (2021)*, 3 dB can show the existence of body wave. SNR can be calculated as follows:

$$SNR_{dB} = \log[(P_{co} - P_{pre})/P_{pre}] \quad (2)$$

where P_{co} is the co-seismic power and P_{pre} is the pre-seismic power. Noise power is the pre-seismic power measured before the earthquake. Since the pre-seismic power is the power measured before the earthquake, then the power of the actual signal is obtained as the difference between the measured power and pre-seismic power. For an arbitrary signal, the power is:

$$P_x = \frac{1}{N}\sum_{n=0}^{N-1} x[n]^2 \quad (3)$$

where *N* is the duration of the signal and x *[n]* is the signal.

2.3 Parameter Estimation

Seismic wave TOA can be analysed and obtained by applying the spectrogram in Equation (1) given as follows [2]:

$$TOA, i = \frac{1}{f}\arg\{\max(\gamma\rho_{x,i}[n,k])\} \quad (4)$$

where γ is the peak reference level of the TFR to estimate TOA. If the half power point is used as a reference, then the reference level γ should be selected as 0.5 [17].

From the TOA estimated from Equation (4), the path velocity can be calculated as:

$$v_{p,i} = d_i/TOA_i \quad (5)$$

where d_i is the range between the epicenter to the *i*-th GPS CORS.

3.0 RESULTS AND ANALYSIS

This section shows result and analysis for estimating seismic wave TOA and path velocity.

3.1 Coordinates Time Series

CTS is presented from the day of 26 December 2004 with the time length of 05 to 1.5 UT that captured the co-seismic activity. The result showed that it was capable to identify a drastic co-seismic displacement at GPS CORS during the earthquake. Figure 3 and Figure 4 show kinematic displacement GPS CORS at BKPL and JHJY in northing and easting components, respectively.

From the CTS, there are still systematic fluctuations that might be caused by error in satellite clocks and orbits fixed in processing and by other environment errors [29]. Therefore, only horizontal components were analysed and vertical components were excluded. It is because the CTS result showed fluctuations and unstable measurements in vertical components. By removing these components, the quality of estimated TOA and path velocity can be improved. Based on related work on measuring seismic wave, the vertical components are nosier and prone to more systematic errors than horizontal [19]. The vertical components were not applied due to poor accuracy compared to horizontal components that were used in estimating the TOA [36].

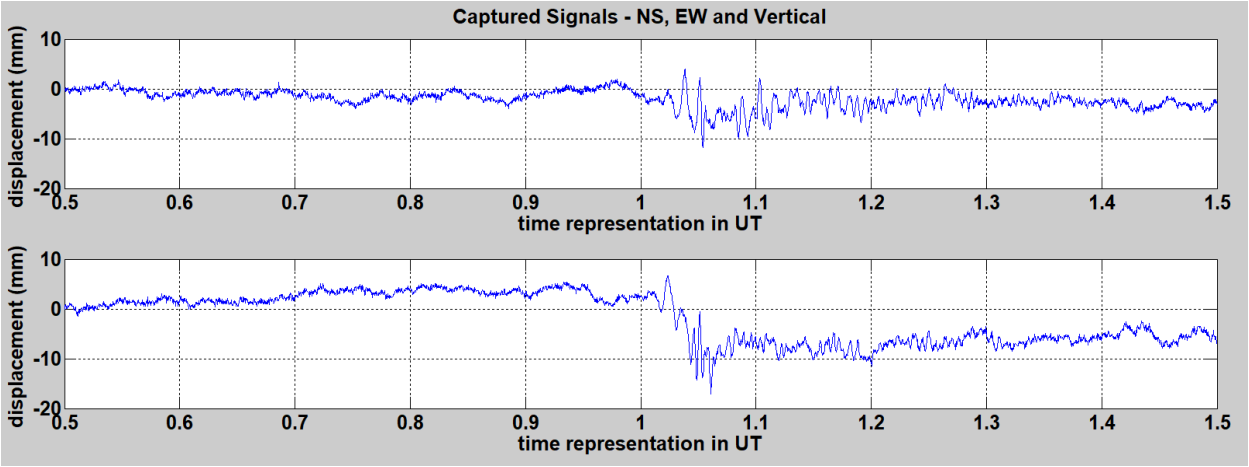

Figure 3 CTS at GPS CORS BKPL

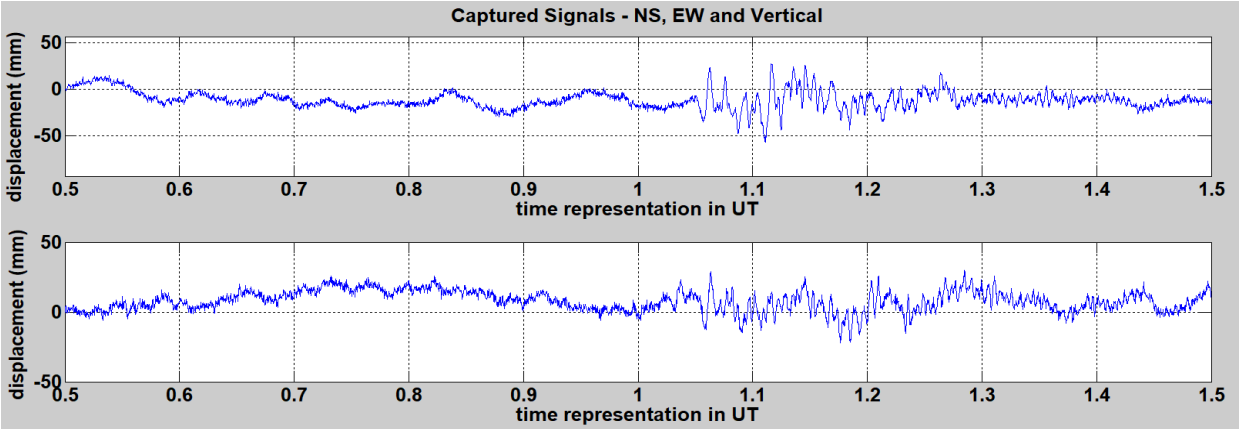

Figure 4 CTS at GPS CORS JHJY

By analysing the displacement from Figure 3 and 4, GPS CORS displacement at BKPL in northern part were about 5mm and 6mm in northing and easting respectively, where the distance to the epicenter was 521.153 km and could still be detected. Compared GPS CORS displacement at JHJY in southern part, the displacement was about 4 mm and 3 mm in northing and easting components, respectively. The distance to epicenter was about 887.698 km, which is further from epicenter compared to the BKPL that is closer to epicenter. It can be said that GPS CORS that are closer to epicenter are more likely impressed with the co-seismic activity compared to the further GPS CORS. Previous study also mentioned that this region was affected during the occurrence of Sumatra-Andaman earthquake [34].

3.2 Seismic Wave Time of Arrival Detection

In TFR, TOA was selected according to 50 percent of maximum and minimum magnitude of the waveform. It can be seen that the waveform showed difference of magnitude before and after the arrival of seismic wave. As mentioned from related work on seismic arrival time detection, sudden variation in energy (magnitude) will occur during seismic wave arrival [35]. But, the signal that arrived earlier has a lower value of magnitude compared to signal that arrived later with higher magnitude value.

Selected GPS CORS at BKPL and JHJY showed the captured signals in N-S and E-W dimension obtained from spectrogram described in equation (1). Figure 5 and Figure 6 show contour plot with horizontal axis time in UT (0.9 to 1.2) and vertical axis in frequency (0 to 0.1), respectively. The co-seismic interval in CTS and TFR from these GPS CORS shows the changes of displacement and magnitude during specific time. To indicate the changes of magnitude, TFR shows better visualization and understanding. During co-seismic, the changes occurred at 1.02 UT to 1.06 UT, 1.08 UT to 1.12 UT for N-S dimension and 1.02 UT to 1.04 UT, 1.04 UT to 1.07 UT for E-W dimension at BKPL. Meanwhile, at JHJY, the changes occurred at 1.03 UT to 1.08 UT, 1.10 UT to 1.13 UT for N-S dimension and 1.05 UT to 1.07 UT, 1.08 UT to 1.10 UT for E-W dimension.

In terms of frequency, the frequency ranged from 0.02 Hz to 0.08 Hz from the 1 Hz GPS CORS data. But, there was rate of frequency changes in respect with time. As mentioned by other research, body wave (P and S-wave) frequency ranges up to 2 Hz, while surface wave is within 0.001 Hz to 0.1 Hz in crust and mantle of the earth [8]. According to previous study the frequency of Sumatra-Andaman 9.1 Mw 2004 earthquake was from 0.082 Hz to 0.163 Hz using seismogram [22].

a) N-S dimension b) E-W dimension

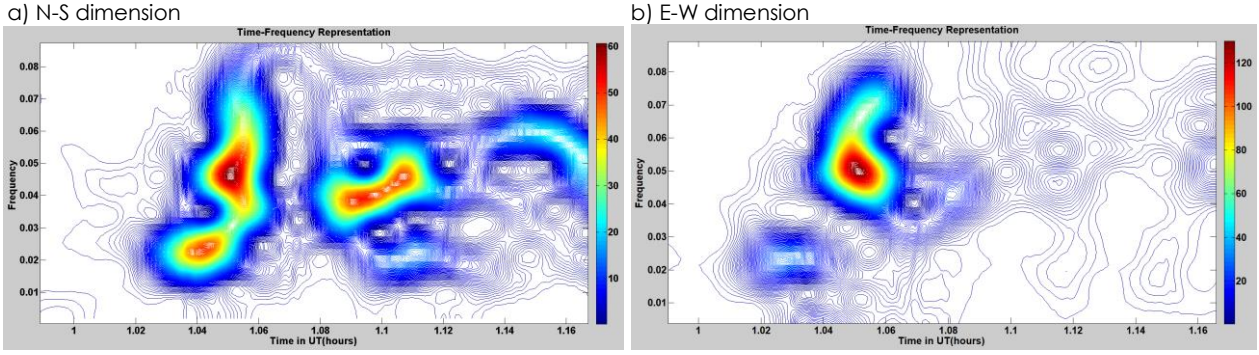

Figure 5 TFR shows GPS CORS in N-S dimension (a) and E-W dimension (b) at BKPL

a) N-S dimension b) E-W dimension

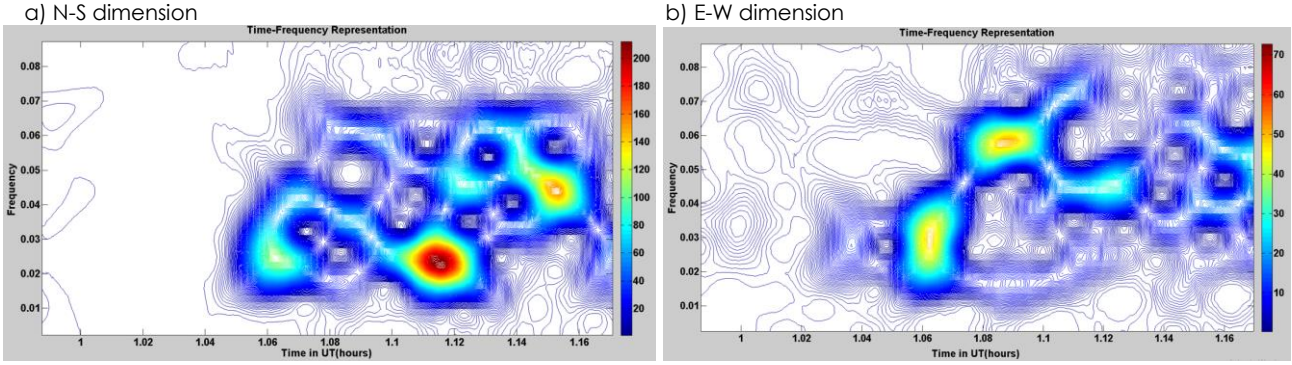

Figure 6 TFR shows GPS CORS in N-S dimension (a) and E-W dimension (b) at JHJY

From the result, it was shown that the changes of magnitude have different types of seismic wave. From Figure 5a, the first peak of magnitude was visible at TOA 1.023 UT with magnitude of 10.00 mm²/s and frequency of 0.02 Hz, while the second peak of magnitude was 60.00 mm²/s and the frequency of 0.05 Hz at TOA was 1.051 UT. Research on determining the seismic wave TOA mentioned that the first wave to appear with small magnitude was P-wave and then S-wave, followed by surface wave; Love wave and Rayleigh wave that consist of higher magnitude [8]. Generally, the surface wave of low-frequency contributes more damage on surface than the body wave of high-frequency during the occurrence of earthquake [15].

It can be said that from this result, S-wave or surface wave can be determined using GPS CORS data but it is difficult to determine P-wave accurately from GPS-only solution because of the significantly less precision [26]. Another reason is because only strong magnitude was observed by GPS CORS in surface. This scenario happened because the GPS CORS pillar installation might not be attached to the bed rock [10, 23] and this is the reason why only strong magnitude was detected. Similar technique was applied to other GPS CORS and the P-wave was not visible, while either the S-wave or surface wave was detected. To further analyse the seismic wave, the S-wave or surface wave was used to determine the TOA and path velocity instead of P-wave.

According to the result, by using equation (4), TOA for GPS CORS at BKPL was detected in N-S and E-W dimensions as 1.0324 UT and 1.0441 UT. Compared to GPS CORS at JHJY, the TOA was about 1.0540 UT and 1.0550 UT in N-S and E-W dimensions, respectively. The difference of TOA between GPS CORS at BKPL and JHJY was because BKPL had a shorter distance to the epicenter (521.153 km) and was likely to receive earliest seismic wave, as compared to JHJY, that was further from epicenter (887.698 km). From the data, it was seen that the TOA was not consistent between each dimension because the propagation of seismic wave at these GPS CORS varies.

The estimated TOA was validated using the SNR obtained from equation (2). For the closer GPS CORS at BKPL, the SNR value was about 9.8 dB and 9.0 dB compared to the value of SNR at JHJY further away from epicenter; 9.8 dB and 6.6 dB in N-S and E-W dimensions, respectively. The result shows that TOA can be validated using the value of SNR. The average SNR values for all selected GPS CORS were between 5.5 dB to 11.9 dB which is quite high and in fact should be higher so as to reduce the estimation error. The result of TOA and SNR is summarized in Table 3.

Table 3 Detection result seismic wave TOA and SNR

Region	GPS CORS	Epicenter Distance (km)	Estimated TOA (UT)		SNR (dB)	
			North	East	North	East
Region 1	BKPL	521.153	1.03240	1.04410	9.8994	9.0535
	SELM	563.954	1.03540	1.04720	9.6145	8.8850
	SGPT	562.777	1.03530	1.04710	11.953	11.993
	BABH	540.448	1.03356	1.04570	11.950	11.548
Region 2	PUPK	517.781	1.03480	1.04390	9.2192	7.0177
	JUIP	584.593	1.04000	1.04880	10.958	9.1335
Region 3	MERU	602.364	1.03750	1.04540	7.0120	4.6334
	BANT	618.741	1.03790	1.04280	9.4518	6.3961
	UPMS	637.997	1.03820	1.04510	7.2789	6.5462
	KKBH	630.548	1.03710	1.04520	10.693	7.1388
Region 4	KUKP	856.253	1.05120	1.05400	8.1717	4.4538
	JHJY	887.698	1.05400	1.05500	9.8247	6.6697
	TGPG	952.339	1.05680	1.05690	7.1388	6.4623

3.3 Estimation on Path Velocity

Further analysis on the waveform of co-seismic GPS CORS at BKPL and JHJY was investigated. From previous TOA result, the path velocity can be estimated based on equation (5), because the epicenter distance and TOA parameter were achieved. As shown in Table 4, the seismic wave of path velocity estimated at GPS CORS BKPL and SELM were 3.8753 km/s and 3.8721 km/s, which is consistent because this GPS CORS is from the same region. From this result, it was shown that the theoretical the seismic surface wave velocity value ranged between 2 km/s to 5 km/s. [4]

Comparing the result with other region, the seismic wave of path velocity determined by other 4 GPS CORS PUPK, MERU, KUKP and JHJY were 3.7046 km/s, 4.0738 km/s, 4.5250 km/s and 4.5248 km/s which vary because of different regions that may have different subsurface of earth surface. According to other study, the subsurface of the earth will influence the seismic wave velocity depending on its physical properties such as rock, soil and mineral [26]. Generally, seismic wave velocity propagates on solid material much faster compared to liquid material [25].

Table 4 Estimated of path velocity

Region	GPS CORS	Epicenter Distance (km)	Averaged Estimated TOA (UT)	Averaged Estimated TOA (s)	Estimated Path Velocity (km/s)
Region 1	BKPL	521.153	1.03825	137.700	3.8753
	SELM	563.954	1.04130	148.680	3.8721
	SGPT	562.777	1.04120	148.320	3.8738
	BABH	540.448	1.03963	142.668	3.8792
Region 2	PUPK	517.781	1.03935	141.660	3.7046
	JUIP	584.593	1.04440	159.840	3.6937
Region 3	MERU	602.364	1.04145	149.220	4.0738
	BANT	618.741	1.04035	145.260	4.2753
	UPMS	637.997	1.04165	149.940	4.2844
	KKBH	630.548	1.04115	148.140	4.2981
Region 4	KUKP	856.253	1.05260	189.360	4.5250
	JHJY	887.698	1.05450	196.200	4.5248
	TGPG	952.339	1.05685	204.660	4.6533

Table 4 also shows that the seismic waves velocity increased from 3.8753 km/s to 4.6533 km/s as the epicenter distance increased from 517.781 km to 952.339 km. This phenomenon can be related to the type and state of the rocks and minerals composing the subsurface of the earth [7]. Another reason was due to the temperature and density of subsurface that might increase or decrease the seismic wave velocity [15, 25]. Overall, this result suggests GPS CORS has successfully captured the S-wave or surface wave signal.

4.0 CONCLUSION

GPS has become an alternative tool to compete with seismometer because of its availability, accuracy and cost effectiveness. The detection of TOA and estimated path velocity is essential to be used in locating epicenter or other geohazard management such as earthquake early warning system. From the study, this research provides an efficient and possible method to estimate the parameter for 2004 Sumatra-Andaman earthquake using 1-Hz GPS derived seismic signal. GPS station displacement can be determined using CTS, and TOA can be determined using TFR. Therefore, the seismic path velocity can be estimated using this parameter. It is shown that TFR is a useful technique to detect TOA in the time-frequency domain.

The path velocity detected by 4 nearest GPS CORS BKPL, SELM, SGPT and BABH with same region were within the range of 3.8753 km/s to 3.8792 km/s with consistent value, suggesting S-wave or surface wave signal can be captured by applying this technique. The existence of P-wave signals may not be seen in CTS because different characteristics of the earth's surface may affect the propagation of seismic wave energy. For GPS, it is challenging to analyse the P-wave arrival because most of GPS CORS have relatively low SNR of waveform. However, it may be possible using more high-rate GPS with 5-Hz or 10-Hz rate data to detect seismic body wave. Moreover, the far field data have successfully captured the seismic wave with distance over 521.153 km from the epicenter.

This work may be of help in estimating parameter. For our future work, the technique that has been discussed will be applied on locating earthquake epicenter. It subsists better to use this method for other major earthquakes such as 2005 Nias-Simeulue earthquake and 2012 Indian Ocean earthquake.

Conflicts of Interest

The author(s) declare(s) that there is no conflict of interest regarding the publication of this paper.

Acknowledgement

The authors thank the Universiti Teknologi Malaysia for funding through the UTM Fundamental Research Grant Vot Q.J130000.3852.22H47, the Department of Survey and Mapping Malaysia (DSMM) for providing the GPS/GNSS data, the Faculty of Built Environment and Surveying, Universiti Teknologi Malaysia and School of Electrical Engineering, Faculty of Engineering for providing the facilities to conduct this study.

References

[1] Amirrudin, Muhammad & Md Din, Ami Hassan & Zulkifli, Nur Adilla & Che Amat, Asyran & Hamden, Mohammad. 2020. Assessment of the Accuracy and Precision of Myrtknet Real-time Services. *Jurnal Teknologi*. 83: 93-103. Doi: 10.11113/jurnalteknologi.v83.13892.

[2] B. Boashash. 2015. *Time-frequency Signal Analysis and Processing*. 2nd Edition. A Comprehensive Reference, Elsevier, Amsterdam.

[3] Blewitt, G., Hammond, W. C., Kreemer, C., Plag, H.-P., Stein, S., & Okal, E. 2009. GPS for Real-time Earthquake Source Determination and Tsunami Warning Systems. *Journal of Geodesy*. 83(3-4): 335-343. Doi: 10.1007/s00190-008-0262-5.

[4] Braile, L. 2004. *Exploration in Earth Science*. Web.ics.purdue.edu. https://web.ics.purdue.edu/~braile/edumod/waves/WaveDemo.htm.

[5] Chen, K., Ge, M., Babeyko, A., Li, X., Diao, F., & Tu, R. 2016. Retrieving Real-time Co-seismic Displacements using GPS/GLONASS: A Preliminary Report from the September 2015Mw8.3 Illapel Earthquake in Chile. *Geophysical Journal International*. 206(2): 941-953. Doi: 10.1093/gji/ggw190.

[6] Chlieh, M., Avouac, J.-P., Hjorleifsdottir, V., Song, T.-R. A., Ji, C., Sieh, K., … Galetzka, J. 2007. Coseismic Slip and Afterslip of the Great Mw 9.15 Sumatra-Andaman Earthquake of 2004. *Bulletin of the Seismological Society of America*. 97(1A): S152-S173. Doi: 10.1785/0120050631.

[7] Cormier, V. F. 1989. Seismic Attenuation: Observation and Measurement. *Geophysics. Encyclopedia of Earth Science*. Springer, Boston, MA. https://doi.org/10.1007/0-387-30752-4_122.

[8] Cormier, V. F. 2015. Treatise on Geophysics. Theory and Observations: Forward Modeling: Synthetic Body Wave Seismograms. 201-230. Doi: 10.1016/B978-0-444-53802-4.00005-1.

[9] EarthScope Consortium. 2021. SAGE: Data Services. Seismological Facility for the Advancement of Geoscience. Retrieved August 24, 2021, from http://ds.iris.edu/ds.

[10] Dixon, Timothy & Mao, Ailin & Bursik, Marcus & Heflin, M. & Langbein, John & Stein, Ross & Webb, Frank. 1997. Continuous Monitoring of Surface Deformation at Long Valley Caldera, California, with GPS. *Journal of Geophysical Research*. 1021: 12017-12034. 10.1029/96JB03902.

[11] Endra Gunawan, Putra Maulida, Irwan Meilano, Masyhur Irsyam, Joni Efendi. 2016. Analysis of Coseismic Fault Slip Models of the 2012 Indian Ocean Earthquake: Importance of GPS Data for Crustal Deformation Studies. *Acta Geophys*. 64(6): 2136-2150.

[12] Fang, R., Shi, C., Song, W., Wang, G., & Liu, J. 2013. Determination of Earthquake Magnitude using GPS Displacement Waveforms from Real-time Precise Point Positioning. *Geophysical Journal International*. 196(1): 461-472. Doi: 10.1093/gji/ggt378.

[13] Geng, T., Xie, X., Fang, R., Su, X., *et al.* 2016. Real-time Capture of Seismic Waves using High-rate Multi-GNSS Observations: Application to the 2015 Mw7.8 Nepal Earthquake. Geophys. *Res. Lett.* 43: 161-167.

[14] Scripps Institution of Oceanography. 1986. Global Seismograph Network - IRIS/IDA [Data set]. International Federation of Digital Seismograph Networks. Retrieved August 24, 2021, from https://doi.org/10.7914/SN/II.

[15] Hays, w. w. 1994. Facing Geologic and Hydrologic Hazards: Earth-science Considerations. Professional Paper. https://pubs.er.usgs.gov/publication/pp1240B. Doi: 10.3133/pp1240B.

[16] Incorporated Research Institutions for Seismology (IRIS). 2021. How are Earthquakes Located? Seismological Facility for the Advancement of Geoscience. Retrieved August 24, 2021, from https://www.iris.edu/hq/inclass/fact-sheet/how_are_earthquakes_located.

[17] J. G. Proakis, D. K. Manolakis. 2013. *Digital Signal Processing*. 4th Edition. Pearson.

[18] Jin, S., & Su, K. 2019. Co-seismic Displacement and Waveforms of the 2018 Alaska Earthquake from High-rate GPS PPP Velocity Estimation. *Journal of Geodesy*. Doi: 10.1007/s00190-019-01269-3.

[19] Kiyoung Kim, Jaemook Choi, Junyeon Chung, Gunhee Koo, In-Hwan Bae, Hoon Sohn. 2018. Structural Displacement Estimation through Multi-rate Fusion of Accelerometer and RTK-GPS Displacement and Velocity Measurements. Measurement. 130: 223-235.

[20] Larson, K. M., Bilich, A., & Axelrad, P. 2007. Improving the precision of high-rate GPS. *Journal of Geophysical Research*. 112(B5). Doi: 10.1029/2006jb004367.

[21] Li, Xingxing. 2015. Real-time High-rate GNSS Techniques for Earthquake Monitoring and Early Warning. 10.14279/depositonce-4585.

[22] Monika Wilde-Piórko; Seweryn J. Duda; Marek Grad. 2011. Frequency Analysis of the 2004 Sumatra-Andaman Earthquake using Spectral Seismograms. *59*(3): 483-501. Doi: 10.2478/s11600-011-0010-8.

[23] Nyberg, S., Kallio, U., Koivula, H. 2013. GPS Monitoring of Bedrock Stability at Olkiluoto Nuclear Waste Disposal Site in Finland from 1996 to 2012. *Journal of Geodetic Science*. 3(2). Doi: 10.2478/jogs-2013-0017.

[24] SAGE. 2021. Query to view seismic stations on the map. Seismological Facility for the Advancement of Geoscience. Retrieved August 24, 2021, from https://ds.iris.edu/gmap/.

[25] Rajasekaran, S. 2009. Structural Dynamics of Earthquake Engineering. Earthquake and Earthquake Ground Motion. 571-604. Doi: 10.1533/9781845695736.2.571.

[26] Schmitt, D. R. 2015. Treatise on Geophysics. Geophysical Properties of the Near Surface Earth: Seismic Properties. 43-87. Doi:10.1016/B978-0-444-53802-4.00190-1.

[27] Sha'ameri, Ahmad Zuri and Wan Aris, Wan Anom and Sadiah, Shahidatul and Musa, Tajul Ariffin. 2021a. GPS Derived Seismic Signals for Far Field Earthquake Epicenter Location Estimation. *Journal of Engineering Technology and Applied Physics*. 3(1): 7-12.

[28] Sha'ameri, A., Wan Aris, W., Sadiah, S. and Musa, T. 2021b. Reliability of Seismic Signal Analysis for Earthquake Epicenter Location Estimation Using 1 Hz GPS Kinematic Solution. *Measurement*. 182: 109669.

[29] Shi, C., Lou, Y., Zhang, H., Zhao, Q., Geng, J., Wang, R., … Liu, J. 2010. Seismic Deformation of the Mw 8.0 Wenchuan Earthquake from High-rate GPS Observations. Advances in Space Research. 46(2): 228-235. Doi: 10.1016/j.asr.2010.03.006.

[30] Shuanggen Jin, Ke Su. 2019. Alaska Earthquake from High-rate GPS PPP Velocity Estimation. *J. Geod.* 93(9): 1559-1569.

[31] Spiller, F. C. P. 1998. Radiolarian Biostratigraphy of Peninsular Malaysia and Implications for Regional Palaeotectonics and Palaeogeography. PhD Thesis

Doctoral. University of New England. https://hdl.handle.net/1959.11/10916.
[32] Pacific Coastal and Marine Science Center. 2018. Tsunami Generation from the 2004 M=9.1 Sumatra-Andaman Earthquake | U.S. Geological Survey. Retrieved August 24, 2021, from https://www.usgs.gov/centers/pcmsc/science/tsunami-generation-2004-m91-sumatra-andaman-earthquake.
[33] Wang, J., Xiao, Z., Liu, C., Zhao, D., & Yao, Z. 2019. Deep Learning for Picking Seismic Arrival Times. *Journal of Geophysical Research: Solid Earth*. Doi: 10.1029/2019jb017536.
[34] W. A. W. Aris. 2018. Spatio-Temporal Crustal Deformation Model of Sundaland in Malaysia Using Global Positioning System. PhD. Thesis. Faculty of Build Environment and Survey, Universiti Teknologi Malaysia.
[35] Xiang, Y., Yue, J., Tang, K., & Li, Z. 2018. A Comprehensive Study of the 2016 Mw 6.0 Italy Earthquake based on High-rate (10 Hz) GPS Data. *Advances in Space Research*. 63(1): 103-117. Doi: 10.1016/j.asr.2018.08.027.
[36] Xiang, Yunfei, Yue, Jianping, Cai, Dongjian, Wang, Hao. 2019. Rapid Determination of Source Parameters for the 2017 Mw 8.2 Mexico Earthquake based on High-rate GPS Data. *Advances in Space Research*. 64(5): 1148-1159. Doi: 10.1016/j.asr.2019.06.001.
[37] Xiao, Dongsheng, Chang, Ming, Su, Yong, Hu, Qijun, Yu, Bing. 2016. Quasi-real Time Inversion Method of Three-dimensional Epicenter Coordinate, Trigger Time, and Magnitude based on CORS. *Earthquake Engineering and Engineering Vibration*. 15(3): 425-433. Doi: 10.1007/s11803-016-0333-.
[38] Yong, C. Z. 2019. Tectonic Geodesy: An Analysis of the Crustal Deformation of the Western Sundaland Plate from Nearly Two Decades of continuous GPS Measurements. Thesis, Doctor of Philosophy. University of Otago. Retrieved December 3, 2019, from http://hdl.handle.net/10523/9484.